Sensitivity Analysis and Optimal Control for Nipah Virus Outbreak

Binti Mualifatul Rosydah[1,2], Marsudi[1*], Wuryansari Muharini Kusumawinahyu[1], Nur Shofianah[1]

[1]Department of Mathematics, Universitas Brawijaya, Malang 65145, Indonesia
[2]Safety Engineering, Politeknik Perkapalan Negeri Surabaya, Surabaya 60111, Indonesia

[*]Email: marsudi61@ub.ac.id

Abstract

Nipah virus (NiV) is a zoonotic pathogen capable of causing outbreaks with high mortality rates, ranging from 40% to 75%. The virus spreads through direct contact between humans and infected animals, consumption of contaminated food, and human-to-human transmission. As no vaccine or specific treatment is currently available, effective control measures must rely on public health policies. In this study, we develop a mathematical model to examine the transmission dynamics of the Nipah virus. We calculate the basic reproduction number R_0 as an indicator of disease spread, perform a sensitivity analysis of key model parameters, and evaluate the effectiveness of three control strategies: health campaigns targeting exposed individuals, quarantine of infected individuals, and treatment to increase the recovery rate. The objective is to minimize both the number of exposed and infected individuals and the overall cost of implementing these controls. The model used is a compartmental framework dividing the human population into five subgroups: susceptible (S), exposed (E), infected (I), recovered (R), and deceased (D). To identify the optimal intervention strategy, we apply the Pontryagin Maximum Principle (PMP), and the resulting optimality system is solved numerically using the Forward–Backward Sweep method. The results show that the effective contact rate, incubation period, and treatment rate are the most influential parameters in determining disease transmission. Sensitivity analysis indicates that reducing R_0 is most effectively achieved by improving the efficiency of health campaigns and treatment. Numerical simulations further demonstrate that the optimal combination of all three control strategies significantly reduces both exposed and infected populations compared with implementing any single strategy alone. With an optimally designed set of interventions, the resulting policy achieves a balance between controlling viral spread and ensuring cost efficiency.

Keywords: Nipah virus, mathematical model, basic reproduction number, sensitivity analysis, optimal control
2020 MSC classification number: 92D30, 37N25, 93C95, 93A30

1. INTRODUCTION

Nipah virus (NiV) is a zoonotic pathogen capable of spilling over from animals to humans. Transmission occurs through direct contact with infected animals, consumption of contaminated food, and human-to-human transmission via respiratory droplets or close physical interaction [10]. The virus was first identified in 1998 in Sungai Nipah, Negeri Sembilan, Malaysia [8], [11], and subsequently caused outbreaks in Singapore [24], Bangladesh [13], [18], [21], [25], the Philippines [6], and India [1], [2], [5], [12], [23], [27], with case fatality rates ranging from 40–75% [31]. The 2018 outbreak in Kerala, India, which reported 23 cases with 21 fatalities [1], provides a crucial validation dataset for mathematical models due to its detailed epidemiological documentation. Given its high mortality rate and the absence of an effective vaccine or specific antiviral therapy, the development of evidence-based public health interventions remains essential for mitigating both health and economic impacts.

Mathematical modelling provides a rigorous framework for understanding the mechanisms governing Nipah virus transmission and for quantitatively assessing disease control strategies. Dynamic compartmental models are central tools in mathematical epidemiology, as they allow for the analysis of disease burden, the prediction of epidemic trajectories, and the estimation of threshold quantities such as the basic reproduction number $\mathcal{R}_0$, which determines whether an infection can invade or die out in a population [14].

The present study extends the modelling frameworks introduced by Zewdie and Gakkhar [32], Raza et al. [26], and Khan et al. [15] by incorporating two important features: transmission resulting from contact

[*]Corresponding Author
Received March 22nd, 2025, Revised November 25th, 2025, Accepted for publication February 20th, 2026.
Published by Indonesian Biomathematical Society, e-ISSN: 2549-2896, DOI:10.5614/cbms.2026.9.1.5

with infected corpses, as emphasized in [32], and an explicit incubation period for exposed individuals, as highlighted in [26]. These additions motivate the introduction of the E compartment, forming an extended $SEIRD$ (Susceptible–Exposed–Infected–Recovered–Deceased) model that more accurately captures the observed epidemiological characteristics of Nipah virus.

Sensitivity analysis plays a crucial role in identifying parameters that exert the greatest influence on disease dynamics and on $\mathcal{R}_0$. By determining which biological processes most strongly affect transmission such as spillover contact rates, human-to-human transmission efficiency, and the recovery rate, public health interventions can be designed to target the most impactful components of the system.

Several previous studies have explored a range of control measures, including public awareness campaigns [15], [17], [22], [30], treatment and clinical management [15], [17], [30], isolation and quarantine protocols [15], [33], rapid diagnostic testing, safe burial practices [22], lifestyle improvements [17], culling of infected animals, and environmental or behavioral interventions such as restricting the collection of date palm sap [33]. While these studies provide valuable insights, most consider only one or two interventions at a time or focus on local outbreak contexts.

In contrast, the present work evaluates multiple simultaneous control strategies, health campaigns for exposed individuals, quarantine of infected individuals, and treatment to enhance recovery within a unified optimal control framework. By integrating epidemiological dynamics with cost considerations, this study seeks to identify intervention strategies that are not only effective in reducing infection prevalence but also feasible and sustainable under realistic resource constraints. The optimal control methodology, combined with numerical simulation, provides actionable guidance for policymakers in designing comprehensive and cost-efficient outbreak responses.

The remainder of this paper is structured as follows. Section 2 introduces the $SEIRD$ model and outlines the underlying assumptions. Section 3 presents the equilibrium analysis, the computation of the basic reproduction number, the sensitivity analysis, and the formulation of the optimal control problem. Section 4 provides the numerical approach and simulation results illustrating the impact of each control strategy with real outbreak data. Section 5 concludes with a summary of the main findings and discusses their practical implications for real-world public health planning.

2. MODEL FORMULATION

The transmission dynamics of the Nipah virus are investigated using a deterministic compartmental model that partitions a homogeneous population into five distinct classes: the susceptible population (S), the exposed population (E), who are infected but not yet infectious, the symptomatic and infectious population (I), the recovered population (R), and the deceased individuals whose bodies remain infectious (D). The model is constructed based on the following core assumptions. Individuals enter the susceptible compartment at a constant recruitment rate Λ, and experience a natural death rate μ across all compartments.

The force of infection arises from two primary sources: direct contact with infectious individuals (I) at a rate β_1, and contact with infected corpses (D) at a rate β_2, with a scaling factor κ representing their relative infectiousness. Intervention strategies mitigate the effective transmission. Public awareness campaigns (e.g., promoting hygiene and avoiding reservoir hosts) reduce the risk of infection from both sources by a factor of $(1-\phi_1)$, while the quarantine of symptomatic individuals reduces transmission from the infectious compartment I by a factor of $(1-\phi_2)$.

Following exposure, individuals progress to the infectious class at a rate γ, although a proportion of exposed individuals recover without developing severe symptoms, transitioning directly to the recovered class at a rate ω. Infectious individuals either recover at a rate η or die from the disease at a rate δ, reflecting the high case fatality rate associated with Nipah virus infection. Recovery is assumed to confer temporary immunity, which wanes at a rate θ, allowing recovered individuals to return to the susceptible class.

Finally, individuals who die in the infectious compartment due to both disease-induced mortality (δ) and natural mortality (μ) contribute to the pool of infectious corpses (D), which are subsequently removed through safe burial practices at a rate α. The transitions among these compartments are governed by the following system of nonlinear ordinary differential equations:

$$\begin{aligned}
\frac{dS}{dt} &= \Lambda - \frac{\beta_1(1-\phi_1)(1-\phi_2)I + \kappa\beta_2(1-\phi_1)D}{N}S - \mu S + \theta R,\\
\frac{dE}{dt} &= \frac{\beta_1(1-\phi_1)(1-\phi_2)I + \kappa\beta_2(1-\phi_1)D}{N}S - (\mu+\gamma+\omega)E,\\
\frac{dI}{dt} &= \gamma E - (\mu+\delta+\eta)I,\\
\frac{dR}{dt} &= \omega E + \eta I - (\mu+\theta)R,\\
\frac{dD}{dt} &= (\mu+\delta)I - \alpha D.
\end{aligned} \tag{1}$$

with initial conditions, $S(0) = S_0 > 0, E(0) = E_0 \geq 0, I(0) = I_0 \geq 0, R(0) = R_0 \geq 0, D(0) = D_0 \geq 0$.

The equation (1) can be expressed in the compartment diagram in Figure 1. The description of parameters in model (1) could be seen in Table 1.

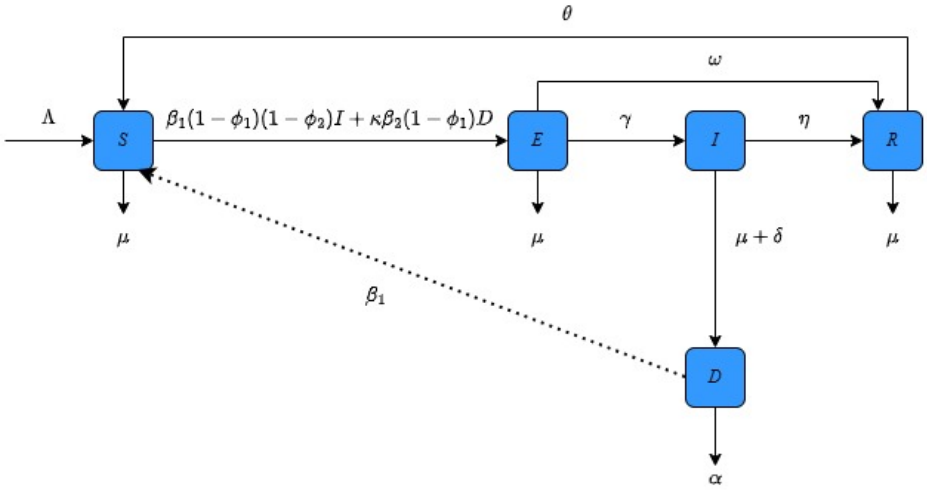

Figure 1: Compartment diagram of the $SEIRD$ model for the spread of Nipah disease.

Table 1: Description of $SEIRD$ model parameters.

Parameter	Description
Λ	Recruitment rate to susceptible class
β_1	Rate of infection from infected individuals
β_2	Rate of infection from dead bodies of infected individuals
κ	Fraction of dead bodies that are handled safely
ϕ_1	Rate of individuals awareness of infectious diseases
ϕ_2	Quarantine rate of infected individuals
γ	Rate of infection in exposed individuals
ω	Rate of recovery in exposed individuals due to awareness
δ	Rate of disease-induced death
η	Rate of recovery in infected individuals due to treatment
θ	Rate of loss of immunity
α	Rate of disposition (burial/cremation) of dead bodies
μ	Natural death rate

3. Model Analysis

3.1. Equilibrium Point

The equilibrium point is obtained when $\frac{dS}{dt} = \frac{dE}{dt} = \frac{dI}{dt} = \frac{dR}{dt} = \frac{dD}{dt} = 0$ [3]. The equilibrium points in the Nipah virus spread model are two, namely the disease-free equilibrium point at

$$E_0 = (S, E, I, R, D) = \left(\frac{\Lambda}{\mu}, 0, 0, 0, 0\right), \tag{2}$$

The disease-free equilibrium point will exist if the condition $I = 0$. Endemic equilibrium point

$$E_1 = (S^*, E^*, I^*, R^*, D^*), \tag{3}$$

such that

$$\begin{aligned}
S^* &= \frac{\alpha N(\mu+\gamma+\omega)(\mu+\delta+\eta)}{\gamma(\alpha\beta_1(1-\phi_1)(1-\phi_2)+\kappa\beta_2(1-\phi_1)(\mu+\delta))},\\
E^* &= \frac{\mu+\delta+\eta}{\gamma}I^*,\\
I^* &= \frac{\alpha\gamma N(\Lambda-\mu S)(\mu+\theta)}{\gamma(\mu+\theta)(\alpha\beta_1(1-\phi_1)(1-\phi_2)+\kappa\beta_2(1-\phi_1)(\mu+\delta))S-\alpha\theta N(\omega(\mu+\delta+\eta)+\eta\gamma)},\\
R^* &= \frac{\omega(\mu+\delta+\eta)+\eta\gamma}{\gamma(\mu+\theta)}I^*,\\
D^* &= \frac{\mu+\delta}{\alpha}I^*.
\end{aligned}$$

3.2. Basic Reproduction Number ($\mathcal{R}_0$)

The basic reproduction number ($\mathcal{R}_0$) is determined by the next generation matrix method [9], [14]. The infectious class of the $SEIRD$ equation is

$$X = \begin{bmatrix} E \\ I \\ D \end{bmatrix}$$

For each infection class, the rate of new infection emergence is indicated by $\mathcal{F}$ and given by

$$\mathcal{F}(X) = \begin{bmatrix} \frac{(\beta_1(1-\phi_1)(1-\phi_2)I+\kappa\beta_2(1-\phi_1)D)S}{N} \\ 0 \\ 0 \end{bmatrix}$$

The other transition rate between infectious classes is denoted by $\mathcal{V}$, which is given by

$$\mathcal{V}(X) = \begin{bmatrix} (\mu+\gamma+\omega)E \\ -\gamma E+(\mu+\delta+\eta)I \\ -(\mu+\delta)I+\alpha D \end{bmatrix}.$$

At disease free equilibrium point the matrice $D\mathcal{F}$ and $D\mathcal{V}$ will give us

$$D\mathcal{F} = \begin{bmatrix} 0 & \beta_1(1-\phi_1)(1-\phi_2) & \kappa\beta_2(1-\phi_1) \\ 0 & 0 & 0 \\ 0 & 0 & 0 \end{bmatrix}.$$

$$D\mathcal{V} = \begin{bmatrix} \mu+\gamma+\omega & 0 & 0 \\ -\gamma & \mu+\delta+\eta & 0 \\ 0 & -(\mu+\delta) & \alpha \end{bmatrix}.$$

Next, the inverse of the matrix $D\mathcal{V}$ is obtained in the form

$$(D\mathcal{V})^{-1} = \begin{bmatrix} \frac{1}{\mu+\gamma+\omega} & 0 & 0 \\ \frac{\gamma}{(\mu+\gamma+\omega)(\mu+\delta+\eta)} & \frac{1}{\mu+\delta+\eta} & 0 \\ \frac{\gamma(\mu+\delta)}{\alpha(\mu+\gamma+\omega)(\mu+\delta+\eta)} & \frac{\mu+\delta}{\alpha(\mu+\delta+\eta)} & \frac{1}{\alpha} \end{bmatrix}.$$

The next-generation matrix is defined as

$$\begin{aligned} K &= (D\mathcal{F})(D\mathcal{V})^{-1} \\ &= \begin{bmatrix} 0 & \beta_1(1-\phi_1)(1-\phi_2) & \kappa\beta_2(1-\phi_1) \\ 0 & 0 & 0 \\ 0 & 0 & 0 \end{bmatrix} \begin{bmatrix} \frac{1}{\mu+\gamma+\omega} & 0 & 0 \\ \frac{\gamma}{(\mu+\gamma+\omega)(\mu+\delta+\eta)} & \frac{1}{\mu+\delta+\eta} & 0 \\ \frac{\gamma(\mu+\delta)}{\alpha(\mu+\gamma+\omega)(\mu+\delta+\eta)} & \frac{\mu+\delta}{\alpha(\mu+\delta+\eta)} & \frac{1}{\alpha} \end{bmatrix} \\ &= \begin{bmatrix} \frac{\gamma(\alpha\beta_1(1-\phi_1)(1-\phi_2)+\kappa\beta_2(1-\phi_1)(\mu+\delta))}{\alpha(\mu+\gamma+\omega)(\mu+\delta+\eta)} & \frac{\alpha\beta_1(1-\phi_1)(1-\phi_2)+\kappa\beta_2(1-\phi_1)(\mu+\delta)}{\alpha(\mu+\delta+\eta)} & \frac{\kappa\beta_2(1-\phi_1)}{\alpha} \\ 0 & 0 & 0 \\ 0 & 0 & 0 \end{bmatrix}. \end{aligned}$$

The basic reproduction number is then calculated as the maximum eigenvalue of the matrix K [4], i.e.

$$\mathcal{R}_0 = \rho(K) = \frac{\gamma(\alpha\beta_1(1-\phi_1)(1-\phi_2) + \kappa\beta_2(1-\phi_1)(\mu+\delta))}{\alpha(\mu+\gamma+\omega)(\mu+\delta+\eta)}. \tag{4}$$

The endemic equilibrium point in (3) can be expressed in $\mathcal{R}_0$ as follows

$$\begin{aligned} S^* &= \frac{N}{\mathcal{R}_0}, \\ E^* &= \frac{\mu+\delta+\eta}{\gamma} I^*, \\ I^* &= \frac{\Lambda(\mathcal{R}_0 - 1)}{\beta_1(1-\phi_1)(1-\phi_2) + \kappa\beta_2(1-\phi_1)\left(\frac{\mu+\delta}{\alpha}\right) - \theta\left(\frac{\omega(\mu+\delta+\eta)+\eta\gamma}{\gamma(\mu+\theta)}\right)\mathcal{R}_0 - \delta}, \\ R^* &= \frac{\omega(\mu+\delta+\eta)+\eta\gamma}{\gamma(\mu+\theta)} I^*, \\ D^* &= \frac{\mu+\delta}{\alpha} I^*. \end{aligned}$$

The endemic equilibrium point will be exists if $\mathcal{R}_0 > 1$.

3.3. Stability Analysis of Equilibrium Point

The stability of the equilibrium point is determined by using linearization of the system of differential equations [28]. The Jacobian matrix of the system (1) is given

$$J = \begin{bmatrix} J_{11} & J_{12} & J_{13} & J_{14} & J_{15} \\ J_{21} & J_{22} & J_{23} & J_{24} & J_{25} \\ 0 & \gamma & -(\mu+\delta+\eta) & 0 & 0 \\ 0 & \omega & \eta & -(\mu+\theta) & 0 \\ 0 & 0 & \mu+\delta & 0 & -\alpha \end{bmatrix}, \tag{5}$$

where

$$
\begin{aligned}
J_{11} &= \frac{-(\beta_1(1-\phi_1)(1-\phi_2)I+\kappa\beta_2(1-\phi_1)D)N+(\beta_1(1-\phi_1)(1-\phi_2)I+\kappa\beta_2(1-\phi_1)D)S}{N^2}-\mu,\\
J_{12} &= \frac{(\beta_1(1-\phi_1)(1-\phi_2)I+\kappa\beta_2(1-\phi_1)D)S}{N^2},\\
J_{13} &= \frac{-\beta_1(1-\phi_1)(1-\phi_2)SN+(\beta_1(1-\phi_1)(1-\phi_2)I+\kappa\beta_2(1-\phi_1)D)S}{N^2},\\
J_{14} &= \frac{(\beta_1(1-\phi_1)(1-\phi_2)I+\kappa\beta_2(1-\phi_1)D)S}{N^2}+\theta,\\
J_{15} &= \frac{-\kappa\beta_2(1-\phi_1)S}{N},\\
J_{21} &= \frac{(\beta_1(1-\phi_1)(1-\phi_2)I+\kappa\beta_2(1-\phi_1)D)N-(\beta_1(1-\phi_1)(1-\phi_2)I+\kappa\beta_2(1-\phi_1)D)S}{N^2},\\
J_{22} &= \frac{-(\beta_1(1-\phi_1)(1-\phi_2)I+\kappa\beta_2(1-\phi_1)D)S}{N^2}-(\mu+\gamma+\omega),\\
J_{23} &= \frac{\beta_1(1-\phi_1)(1-\phi_2)SN-(\beta_1(1-\phi_1)(1-\phi_2)I+\kappa\beta_2(1-\phi_1)D)S}{N^2},\\
J_{24} &= \frac{-(\beta_1(1-\phi_1)(1-\phi_2)I+\kappa\beta_2(1-\phi_2)D)S}{N^2},\\
J_{25} &= \frac{\kappa\beta_2(1-\phi_1)S}{N}.
\end{aligned}
$$

The eigenvalues of the Jacobian matrix J (5) can be used to determine the stability of the equilibrium point.

Theorem 3.1. *Disease-free equilibrium point is locally asymptotically stable under the condition* $\mathcal{R}_0 < 1$.

Proof: The Jacobian matrix of the disease-free equilibrium point is obtained by substituting the disease-free equilibrium point (2) into the Jacobian matrix (5), is given as the following matrix

$$
J(E_0) = \begin{bmatrix} -\mu & 0 & c_1 & \theta & c_2 \\ 0 & c_3 & -c_1 & 0 & -c_2 \\ 0 & \gamma & c_4 & 0 & 0 \\ 0 & \omega & \eta & c_5 & 0 \\ 0 & 0 & c_6 & 0 & -\alpha \end{bmatrix}, \tag{6}
$$

where

$$
\begin{aligned}
c_1 &= -\beta_1(1-\phi_1)(1-\phi_2),\\
c_2 &= -\kappa\beta_2(1-\phi_1),\\
c_3 &= -(\mu+\gamma+\omega),\\
c_4 &= -(\mu+\delta+\eta),\\
c_5 &= -(\mu+\theta),\\
c_6 &= -(\mu+\delta).
\end{aligned}
$$

We get eigenvalue from Jacobian matrix (6) are $\lambda_1 = -\mu, \lambda_2 = -(\mu+\theta)$ and the remaining eigenvalues are the solution of the characteristic polynomial

$$
a_0\lambda^3 + a_1\lambda^2 + a_2\lambda + a_3 = 0,
$$

where

$$
\begin{aligned}
a_0 &= 1,\\
a_1 &= \alpha - c_4 - c_3,\\
a_2 &= -\alpha c_4 - \alpha c_3 - c_3 c_4 + \gamma c_1,\\
a_3 &= \alpha c_3 c_4 + \alpha\gamma c_1 + \gamma c_2 c_6.
\end{aligned}
$$

By applying Routh-Hurwirtz criteria for 3rd order [17], $a_0 > 0, a_1 > 0, b_1 = \frac{a_1 a_2 - a_0 a_3}{a_1} > 0$ and $a_3 > 0$.

$$
\begin{aligned}
&a_3 > 0,\\
&1 > \frac{\alpha\gamma\beta_1(1-\phi_1)(1-\phi_2) + \gamma\kappa\beta_2(1-\phi_1)(\mu+\delta)}{\alpha(\mu+\gamma+\omega)(\mu+\delta+\eta)},\\
&1 > \mathcal{R}_0.
\end{aligned}
$$

Hence, disease-free equilibrium point is locally asymptotically stable if $\mathcal{R}_0 < 1$. ■

Theorem 3.2. *The endemic equilibrium point* (E_1) *is locally asymptotically stable if* $\mathcal{R}_0 > 1$.

Proof: The Jacobian matrix of the endemic equilibrium point is obtained by substituting the endemic equilibrium point (3) into the Jacobian matrix (5), resulting in the following matrix:

$$
J(E_1) = \begin{bmatrix} d_1 & d_2 & d_3 & d_4 & d_5 \\ d_6 & d_7 & d_8 & d_9 & d_10 \\ 0 & \gamma & c_4 & 0 & 0 \\ 0 & \omega & \eta & c_5 & 0 \\ 0 & 0 & c_6 & 0 & -\alpha \end{bmatrix}, \tag{7}
$$

where

$$
\begin{aligned}
d_1 &= \frac{-(\beta_1(1-\phi_1)(1-\phi_2)I^* + \kappa\beta_2(1-\phi_1)D^*)N + (\beta_1(1-\phi_1)(1-\phi_2)I^* + \kappa\beta_2(1-\phi_1)D^*)S^*}{N^2} - \mu,\\
d_2 &= \frac{(\beta_1(1-\phi_1)(1-\phi_2)I^* + \kappa\beta_2(1-\phi_1)D^*)S^*}{N^2},\\
d_3 &= \frac{-\beta_1(1-\phi_1)(1-\phi_2)S^*N + (\beta_1(1-\phi_1)(1-\phi_2)I^* + \kappa\beta_2(1-\phi_1)D^*)S^*}{N^2},\\
d_4 &= \frac{(\beta_1(1-\phi_1)(1-\phi_2)I^* + \kappa\beta_2(1-\phi_1)D^*)S^*}{N^2} + \theta,\\
d_5 &= \frac{-\kappa\beta_2(1-\phi_1)S^*}{N},\\
d_6 &= \frac{(\beta_1(1-\phi_1)(1-\phi_2)I^* + \kappa\beta_2(1-\phi_1)D^*)N - (\beta_1(1-\phi_1)(1-\phi_2)I^* + \kappa\beta_2(1-\phi_1)D^*)S^*}{N^2},\\
d_7 &= \frac{-(\beta_1(1-\phi_1)(1-\phi_2)I^* + \kappa\beta_2(1-\phi_1)D^*)S^*}{N^2} - (\mu+\gamma+\omega),\\
d_8 &= \frac{\beta_1(1-\phi_1)(1-\phi_2)S^*N - (\beta_1(1-\phi_1)(1-\phi_2)I^* + \kappa\beta_2(1-\phi_1)D^*)S^*}{N^2},\\
d_9 &= \frac{-(\beta_1(1-\phi_1)(1-\phi_2)I^* + \kappa\beta_2(1-\phi_2)D^*)S^*}{N^2},\\
d_{10} &= \frac{\kappa\beta_2(1-\phi_1)S^*}{N}.
\end{aligned}
$$

The characteristic polynomial of matrix (7) is given by

$$
a_0\lambda^5 + a_1\lambda^4 + a_2\lambda^3 + a_3\lambda^2 + a_4\lambda + a_5 = 0,
$$

where

$$
\begin{aligned}
a_0 &= 1,\\
a_1 &= \alpha - d_1 - c_5 - d_7 - c_4,\\
a_2 &= c_5d_1 + d_1d_7 + c_4d_1 + c_5d_7 + c_4c_5 + c_4d_7 - \alpha d_1 - \alpha c_5 - \alpha d_7 - \alpha c_4 - \omega d_9 - \gamma d_8 - d_2d_6,\\
a_3 &= \alpha c_5d_1 + \alpha d_1d_7 + \alpha c_4d_1 + \alpha c_5d_7 + \alpha c_4c_5 + \alpha c_4d_7 + \omega d_1d_9 + \gamma d_1d_8 + \omega c_4d_9 + \gamma c_5d_8\\
&\quad + c_5d_2d_6 + c_4d_2d_6 - \alpha\gamma d_8 - \gamma c_6d_{10} - \alpha\omega d_9 - \alpha d_2d_6 - c_5d_1d_7 - c_4c_5d_1 - c_4d_1d_7 - \eta\gamma d_9\\
&\quad - c_4c_5d_7 - \omega d_4d_6 - \gamma d_3d_6,\\
a_4 &= \gamma c_5c_6d_{10} + \gamma c_6d_1d_{10} + \alpha\omega d_1d_9 + \alpha\gamma d_1d_8 + \alpha\omega c_4d_9 + \alpha\gamma c_5d_8 + \alpha c_5d_2d_6 + \alpha c_4d_2d_6\\
&\quad + \eta\gamma d_1d_9 + c_4c_5d_1d_7 + \omega c_4d_4d_6 + \gamma c_5d_3d_6 - \gamma c_6d_5d_6 - \alpha c_5d_1d_7 - \alpha c_4c_5d_1 - \alpha c_4d_1d_7\\
&\quad - \alpha\eta\gamma d_9 - \alpha c_4c_5d_7 - \alpha\omega d_4d_6 - \alpha\gamma d_3d_6 - \omega c_4d_1d_9 - \gamma c_5d_1d_8 - \eta\gamma d_4d_6 - c_4c_5d_2d_6,\\
a_5 &= \gamma c_5c_6d_5d_6 + \alpha\eta\gamma d_1d_9 + \alpha c_4c_5d_1d_7 + \alpha\omega c_4d_4d_6 + \alpha\gamma c_5d_3d_6 - \alpha\omega c_4d_1d_9 - \alpha\gamma c_5d_1d_8\\
&\quad - \alpha\eta\gamma d_4d_6 - \alpha c_4c_5d_2d_6 - \gamma c_5c_6d_1d_{10}.
\end{aligned}
$$

Since the eigenvalues are difficult to determine, we use the Routh-Hurwirtz criteria to determine the stability of the endemic equilibrium point [20].

Table 2: Routh-Hurwirtz criteria for 5th-order.

s^5	a_0	a_2	a_4	0	0
s^4	a_1	a_3	a_5	0	0
s_3	b_1	b_2	0	0	0
s^2	e_1	e_2	0	0	0
s^1	f_1	f_2	0	0	0
s^0	g_1	0	0	0	0

It needs to be shown that $a_0 > 0, a_1 > 0, b_1 = \frac{a_1a_2 - a_0a_3}{a_1} > 0, b_2 = \frac{a_1a_4 - a_0a_5}{a_1} > 0, e_1 = \frac{b_1a_3 - a_1b_2}{b_1} > 0, e_2 = a_5 > 0, f_1 = \frac{e_1b_2 - b_1e_2}{e_1} > 0$ and $g_1 = f_1 > 0$. Since it is difficult to verify analytically the stability condition of the endemic equilibrium point which requires the condition $\mathcal{R}_0 > 1$, it will be verified numerically. ■

3.4. Sensitivity Analysis

Sensitivity analysis is conducted to identify the parameters that exert the greatest influence on the transmission dynamics of the Nipah virus and can therefore serve as a basis for designing effective control strategies. The influence of each parameter is quantified through its sensitivity index with respect to the basic reproduction number $(\mathcal{R}_0)$. A positive sensitivity index indicates that an increase in the corresponding parameter leads to an increase in $\mathcal{R}_0$, with larger positive values reflecting a stronger direct effect on the output. Conversely, a negative sensitivity index indicates that an increase in the parameter results in a decrease in $\mathcal{R}_0$, and larger negative values imply a stronger inverse effect. A sensitivity index equal to, or close to, zero suggests that variations in the parameter have little to no impact on $\mathcal{R}_0$. The sensitivity index is defined as

$$
\Upsilon_p^{\mathcal{R}_0} = \frac{\partial \mathcal{R}_0}{\partial p}\frac{p}{\mathcal{R}_0}, \tag{8}
$$

where p is the parameter being analysed for its effect [7]. Sensitivity index of each parameter in the model (1) will calculated by using Equation (8), we get

$$
\begin{aligned}
\Upsilon_{\gamma}^{R_0} &= \frac{\mu+\omega}{\mu+\gamma+\omega},\\
\Upsilon_{\alpha}^{R_0} &= -\frac{\kappa\beta_2(\mu+\delta)}{\alpha\beta_1(1-\phi_2)+\kappa\beta_2(\mu+\delta)},\\
\Upsilon_{\beta_1}^{R_0} &= \frac{\alpha\beta_1(1-\phi_1)(1-\phi_2)}{\alpha\beta_1(1-\phi_1)(1-\phi_2)+\kappa\beta_2(1-\phi_1)(\mu+\delta)},\\
\Upsilon_{\phi_1}^{R_0} &= -\frac{\phi_1(\alpha\beta_1(1-\phi_2)+\kappa\beta_2(\mu+\delta))}{\alpha\beta_1(1-\phi_1)(1-\phi_2)+\kappa\beta_2(1-\phi_1)(\mu+\delta)},\\
\Upsilon_{\phi_2}^{R_0} &= -\frac{\alpha\beta_1(1-\phi_1)\phi_2}{\alpha\beta_1(1-\phi_1)(1-\phi_2)+\kappa\beta_2(1-\phi_1)(\mu+\delta)},\\
\Upsilon_{\kappa}^{R_0} &= \frac{\kappa\beta_2(1-\phi_1)(\mu+\delta)}{\alpha\beta_1(1-\phi_1)(1-\phi_2)+\kappa\beta_2(1-\phi_1)(\mu+\delta)},\\
\Upsilon_{\beta_2}^{R_0} &= \frac{\kappa\beta_2(1-\phi_1)(\mu+\delta)}{\alpha\beta_1(1-\phi_1)(1-\phi_2)+\kappa\beta_2(1-\phi_1)(\mu+\delta)},\\
\Upsilon_{\mu}^{R_0} &= -\frac{\mu\left(2\alpha\beta_1(\mu+\frac{\omega}{2}+\frac{\eta}{2}+\frac{\delta}{2}+\frac{\gamma}{2})(1-\phi_2)+\kappa\beta_2(\mu^2+2\delta\mu+\delta^2+\eta\delta-\eta(\omega+\gamma))\right)}{(\mu+\gamma+\omega)(\mu+\delta+\eta)(\alpha\beta_1(1-\phi_2)+\kappa\beta_2(\mu+\delta))},\\
\Upsilon_{\delta}^{R_0} &= -\frac{\delta(\alpha\beta_1(1-\phi_2)-\kappa\beta_2\eta)}{(\mu+\delta+\eta)(\alpha\beta_1(1-\phi_2)+\kappa\beta_2(\mu+\delta))},\\
\Upsilon_{\omega}^{R_0} &= -\frac{\omega}{\mu+\gamma+\omega},\\
\Upsilon_{\eta}^{R_0} &= -\frac{\eta}{\mu+\delta+\eta}.
\end{aligned}
$$

The sensitivity analysis, conducted through a Partial Rank Correlation Coefficient (PRCC) assessment, reveals crucial insights into the parameters governing the transmission dynamics of the Nipah virus. The parameter values used in the model are shown in Table 3.

Table 3: Value of parameters.

Parameter	Value	Source
Λ	6295.16	[19]
β_1	1	[19]
β_2	0.651	[32]
κ	0.35	[29]
ϕ_1	0.15	Assumed
ϕ_2	0.15	Assumed
γ	1	[19]
ω	0.09	Fitted
δ	0.771	[33]
η	0.091	[32]
θ	0.851	[32]
α	0.5	[32]
μ	0.16	[19]

The sensitivity analysis as shown in Figure 2. The analysis demonstrates that the transmission rate from infectious individuals (β_1), the corpse transmission scaling factor (κ), and the transmission rate from deceased individuals (β_2) exhibit the strongest positive correlation with the basic reproduction number ($\mathcal{R}_0$), identifying them as the primary drivers of outbreak propagation. Conversely, parameters representing control interventions particularly public awareness (ϕ_1) and quarantine measures (ϕ_2) show significant negative correlations with $\mathcal{R}_0$, highlighting their importance in outbreak containment. The recovery rate of symptomatic individuals (η) also demonstrates a substantial negative correlation, emphasizing the dual benefit of effective treatment in both reducing mortality and limiting transmission.

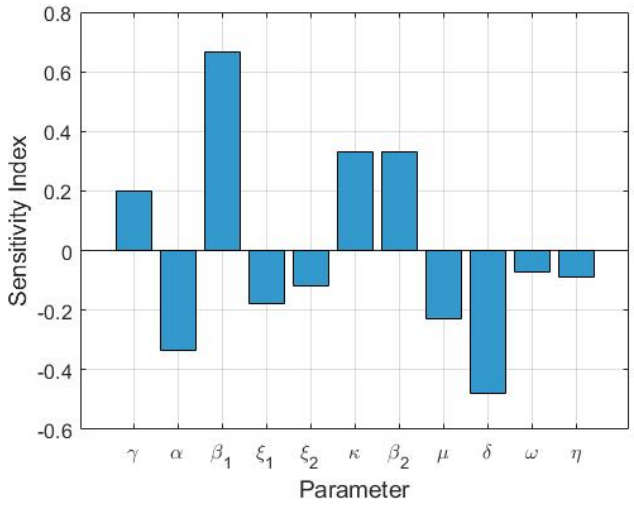

Figure 2: Local sensitivity analysis diagram of $\mathcal{R}_0$.

For policymakers, these findings provide a clear strategic framework for intervention prioritization. The strong positive sensitivity of κ, β_1, and β_2 indicates that the most effective control measures will be those targeting direct transmission pathways. This includes implementing strict safe-burial protocols to reduce corpse-mediated transmission, combined with rapid case isolation and quarantine measures to limit contact with infectious individuals. At the same time, the significant negative sensitivity of ϕ_1 and ϕ_2 underscores the critical importance of sustained public health campaigns that promote personal protective behaviors and early care-seeking, alongside robust contact-tracing systems.

Furthermore, the pronounced effect of the recovery rate (η) justifies strategic investments in healthcare capacity, particularly in supportive care for severe cases, which simultaneously improves clinical outcomes and reduces transmission risk. Overall, this analytical approach provides an evidence-based foundation for resource allocation, emphasizing that an integrated strategy addressing multiple high-sensitivity parameters simultaneously will yield the greatest impact on outbreak control.

3.5. Optimal Control

Based on the results of the sensitivity analysis that has been carried out, it is found that those that affect the spread of the Nipah virus are β_1, κ, and β_2. This can be used as a reason to control the spread of the virus. The possible controls are reducing close contact of susceptible individuals with infected individuals through health campaigns $u_1(t)$, reducing contact with unprotected infected dead bodies through quarantine $u_2(t)$, and treatment control $u_3(t)$, so that the model using control can be expressed in the form of the following differential equation system (9).

$$\begin{aligned}
\frac{dS}{dt} &= \Lambda - \frac{\beta_1(1-u_1)(1-u_2)I + \kappa\beta_2(1-u_1)D}{N}S - \mu S + \theta R,\\
\frac{dE}{dt} &= \frac{\beta_1(1-u_1)(1-u_2)I + \kappa\beta_2(1-u_1)D}{N}S - (\mu+\gamma+\omega)E,\\
\frac{dI}{dt} &= \gamma E - (\mu+\delta+\eta)I - u_3 I,\\
\frac{dR}{dt} &= \omega E + (\eta+u_3)I - (\mu+\theta)R,\\
\frac{dD}{dt} &= (\mu+\delta)I - \alpha D.
\end{aligned} \tag{9}$$

The purpose of this study is to minimize the number of infected individuals as well as reduce the cost required to create awareness and treatment at predetermined time intervals with the objective function is given by

$$J(u_1, u_2, u_3) = \int_0^T \left(A_1 E(t) + A_2 I(t) + \frac{1}{2}\left(B_1 u_1^2 + B_2 u_2^2 + B_3 u_3^2\right) \right) dt, \tag{10}$$

where A_1 and A_2 are the weights of the exposed and infected subpopulations, respectively, B_1, B_2, and B_3 are the weights of the control costs.

Based on the objective function (10) and the constraint system of equations (9), the first step in solving the optimal control problem is to form the Hamiltonian function, from which the optimality system is derived, as follows:

$$\mathcal{H} = A_1 E(t) + A_2 I(t) + \frac{1}{2} B_1 u_1^2 + \frac{1}{2} B_2 u_2^2 + \frac{1}{2} B_3 u_3^2 + \sum_{i=1}^{5} \Upsilon_i f_i, \tag{11}$$

with $\Upsilon_i, i = 1, ..., 5$ representing the costate variable and f_i being the right-hand side of the system of equations (9). The Hamiltonian function (11) can be expressed as follows

$$\begin{aligned}
\mathcal{H} = {} & A_1 E(t) + A_2 I(t) + \frac{1}{2} B_1 u_1^2 + \frac{1}{2} B_2 u_2^2 + \frac{1}{2} B_3 u_3^2 \\
& + \Upsilon_1 \left(\Lambda - \frac{\beta_1 (1-u_1)(1-u_2) I + \kappa \beta_2 (1-u_1) D}{N} S - \mu S + \theta R \right) \\
& + \Upsilon_2 \left(\frac{\beta_1 (1-u_1)(1-u_2) I + \kappa \beta_2 (1-u_1) D}{N} S - (\mu + \gamma + \omega) E \right) \\
& + \Upsilon_3 \left(\gamma E - (\mu + \delta + \eta + u_3) I \right) \\
& + \Upsilon_4 \left(\omega E + (\eta + u_3) I - (\mu + \theta) R \right) \\
& + \Upsilon_5 \left((\mu + \delta) I - \alpha D \right).
\end{aligned} \tag{12}$$

Pontryagin's principle transforms the optimal control problem that minimizes the objective function (10) with the constraint of the differential equation system (9) into a problem of minimizing the Hamiltonian function. After the Hamiltonian function is constructed, the state equations, costate equations, and stationary conditions are determined. Based on Pontryagin's principle, the Hamiltonian function reaches an optimal solution if the state equations, costate equations, and stationary conditions are satisfied [16].

1) State Equation: The state equations are obtained by differentiating the Hamilton function (12) with respect to each costate variable as follows.

$$\begin{aligned}
\frac{dS}{dt} &= \frac{\partial \mathcal{H}}{\partial \Upsilon_1} = \Lambda - \frac{\beta_1 (1-u_1)(1-u_2) I + \kappa \beta_2 (1-u_1) D}{N} S - \mu S + \theta R, \\
\frac{dE}{dt} &= \frac{\partial \mathcal{H}}{\partial \Upsilon_2} = \frac{\beta_1 (1-u_1)(1-u_2) I + \kappa \beta_2 (1-u_1) D}{N} S - (\mu + \gamma + \omega) E, \\
\frac{dI}{dt} &= \frac{\partial \mathcal{H}}{\partial \Upsilon_3} = \gamma E - (\mu + \delta + \eta + u_3) I, \\
\frac{dR}{dt} &= \frac{\partial \mathcal{H}}{\partial \Upsilon_4} = \omega E + (\eta + u_3) I - (\mu + \theta) R, \\
\frac{dD}{dt} &= \frac{\partial \mathcal{H}}{\partial \Upsilon_5} = (\mu + \delta) I - \alpha D.
\end{aligned} \tag{13}$$

with initial conditions $S(0) = S_0, E(0) = E_0, I(0) = I_0, R(0) = R_0, D(0) = D_0$.

2) Costate Equation: The costate equations are the negative values of the derivatives of the Hamiltonian function (12) with respect to each state variable as follows.

$$\begin{aligned}
\frac{d\Upsilon_1}{dt} &= -\frac{\partial \mathcal{H}}{\partial S} \\
&= \Upsilon_1\left(\frac{\beta_1(1-u_1)(1-u_2)I+\kappa\beta_2(1-u_1)D}{N}+\mu\right)-\Upsilon_2\left(\frac{\beta_1(1-u_1)(1-u_2)I+\kappa\beta_2(1-u_1)D}{N}\right), \\
\frac{d\Upsilon_2}{dt} &= -\frac{\partial \mathcal{H}}{\partial E} \\
&= -A_1-\Upsilon_1\left(\frac{\beta_1(1-u_1)(1-u_2)I+\kappa\beta_2(1-u_1)D}{N}\right) \\
&\quad +\Upsilon_2\left(\frac{\beta_1(1-u_1)(1-u_2)I+\kappa\beta_2(1-u_1)D}{N}+(\mu+\gamma+\omega)\right)-\Upsilon_3\gamma-\Upsilon_4\omega, \\
\frac{d\Upsilon_3}{dt} &= -\frac{\partial \mathcal{H}}{\partial I} \\
&= -A_2+\Upsilon_1\left(\frac{\beta_1(1-u_1)(1-u_2)SN-(\beta_1(1-u_1)(1-u_2)I+\kappa\beta_2(1-u_1)D)S}{N^2}\right) \\
&\quad -\Upsilon_2\left(\frac{\beta_1(1-u_1)(1-u_2)SN-(\beta_1(1-u_1)(1-u_2)I+\kappa\beta_2(1-u_1)D)S}{N^2}\right)+\Upsilon_3(\mu+\delta+\eta+u_3) \\
&\quad -\Upsilon_4(\eta+u_3)-\Upsilon_5(\mu+\delta), \\
\frac{d\Upsilon_4}{dt} &= -\frac{\partial \mathcal{H}}{\partial R} \\
&= -\Upsilon_1\left(\frac{\beta_1(1-u_1)(1-u_2)I+\kappa\beta_2(1-u_1)D}{N}+\theta\right)+\Upsilon_2\frac{\beta_1(1-u_1)(1-u_2)I+\kappa\beta_2(1-u_1)D}{N} \\
&\quad +\Upsilon_4(\mu+\theta), \\
\frac{d\Upsilon_5}{dt} &= -\frac{\partial \mathcal{H}}{\partial D} \\
&= \Upsilon_1\frac{\kappa\beta_2(1-u_1)S}{N}-\Upsilon_2\frac{\kappa\beta_2(1-u_1)S}{N}+\Upsilon_5\alpha.
\end{aligned} \tag{14}$$

with transversal conditions $\Upsilon_1(T)=\Upsilon_2(T)=\Upsilon_3(T)=\Upsilon_4(T)=\Upsilon_5(T)=0$.

3) The stationary condition: The stationary condition for the optimal control problem (10) is obtained by the partial derivative of the Hamiltonian function (12) with respect to the control variables u_1, u_2, and u_3, resulting in

$$\begin{aligned}
\frac{\partial \mathcal{H}}{\partial u_1} &= 0, \\
0 &= B_1u_1+\frac{\Upsilon_1(\beta_1(1-u_2)IS+\kappa\beta_2DS)}{N}-\frac{\Upsilon_2(\beta_1(1-u_2)IS+\kappa\beta_2DS)}{N}, \\
\hat{u}_1 &= \frac{(\beta_1(1-u_2)I^*S^*+\kappa\beta_2D^*S^*)(\Upsilon_2-\Upsilon_1)}{B_1N}, \\
\frac{\partial \mathcal{H}}{\partial u_2} &= 0, \\
0 &= B_2u_2+\frac{\Upsilon_1\beta_1(1-u_1)IS}{N}-\frac{\Upsilon_2\beta_1(1-u_1)IS}{N}, \\
\hat{u}_2 &= \frac{\beta_1(1-u_1)I^*S^*(\Upsilon_2-\Upsilon_1)}{B_2N}, \\
\frac{\partial \mathcal{H}}{\partial u_3} &= 0, \\
0 &= B_3u_3-\Upsilon_3I+\Upsilon_4I, \\
\hat{u}_3 &= \frac{(\Upsilon_3-\Upsilon_4)I^*}{B_3}.
\end{aligned}$$

substitution $\hat{u}_1=\frac{(\beta_1(1-u_2)IS+\kappa\beta_2DS)(\Upsilon_2-\Upsilon_1)}{B_1N}$ to $\hat{u}_2$, so that it is obtained

$$\hat{u}_2 = \frac{\beta_1(1-(\frac{(\beta_1(1-u_2)IS+\kappa\beta_2 DS)(\Upsilon_2-\Upsilon_1)}{B_1N}))IS(\Upsilon_2-\Upsilon_1)}{B_2N},$$
$$\hat{u}_2 = \frac{(\beta_1 B_1 N-(\beta_1^2(1-u_2)IS+\kappa\beta_1\beta_2 DS)(\Upsilon_2-\Upsilon_1))IS(\Upsilon_2-\Upsilon_1)}{B_1B_2N^2},$$
$$\hat{u}_2 = \frac{(\beta_1 B_1 N-(\beta_1^2 I^*S^*+\kappa\beta_1\beta_2 D^*S^*)(\Upsilon_2-\Upsilon_1))I^*S^*(\Upsilon_2-\Upsilon_1)}{B_1B_2N^2-\beta_1^2 I^{*2}S^{*2}(\Upsilon_2-\Upsilon_1)}.$$

Substitution $\hat{u}_2$ to $\hat{u}_1$, so that it is obtained

$$\hat{u}_1 = \frac{\left(\beta_1\left(1-\frac{\left(\beta_1 B_1 N-\left(\beta_1^2 I^*S^*+\kappa\beta_1\beta_2 D^*S^*\right)(\Upsilon_2-\Upsilon_1)\right)I^*S^*(\Upsilon_2-\Upsilon_1)}{B_1B_2N^2-\beta_1^2 I^{*2}S^{*2}(\Upsilon_2-\Upsilon_1)}\right)\right)I^*S^*+\kappa\beta_2 D^*S^*(\Upsilon_2-\Upsilon_1)}{B_1N}$$
$$= \frac{W}{B_1N\left(B_1B_2N^2-\beta_1^2 I^{*2}S^{*2}(\Upsilon_2-\Upsilon_1)\right)},$$

where

$$W = \beta_1 B_1 B_2 N^2 - \beta_1^2 I^{*2}S^{*2}(\Upsilon_2-\Upsilon_1) - \left(\beta_1^2 B_1 N - \left(\beta_1^3 I^*S^*+\kappa\beta_1^2\beta_2 D^*S^*\right)(\Upsilon_2-\Upsilon_1)\right)I^*S^*(\Upsilon_2-\Upsilon_1)I^*S^* + \kappa\beta_2 D^*S^*(\Upsilon_2-\Upsilon_1).$$

Control variables in the Nipah virus spread model with health campaigns, quarantine, and treatment are defined as $0 \le u_1 \le 1, 0 \le u_2 \le 1$, and $0 \le u_3 \le 1$, thus obtaining a solution

$$\hat{u}_1^* = \begin{cases} 0, & \text{if } \hat{u}_1 \le 0, \\ \hat{u}_1, & 0 < \hat{u}_1 < 1, \\ 1, & \text{if } \hat{u}_1 \ge 1. \end{cases} \tag{15}$$

$$\hat{u}_2^* = \begin{cases} 0, & \text{if } \hat{u}_2 \le 0, \\ \hat{u}_2, & 0 < \hat{u}_2 < 1, \\ 1, & \text{if } \hat{u}_2 \ge 1, \end{cases} \tag{16}$$

and

$$u_3^* = \begin{cases} 0, & \hat{u}_3 \le 0, \\ \hat{u}_3, & 0 < \hat{u}_3 < 1, \\ 1, & \hat{u}_3 \ge 1, \end{cases} \tag{17}$$

So, the optimal controls $\hat{u}_1^*(t), \hat{u}_2^*(t)$, and $u_3^*(t)$ can be expressed as

$$\hat{u}_1^* = \max\left\{0, \min\left(\frac{W}{B_1N\left(B_1B_2N^2-\beta_1^2 I^{*2}S^{*2}(\Upsilon_2-\Upsilon_1)\right)}, 1\right)\right\},$$
$$\hat{u}_2^* = \max\left\{0, \min\left(\frac{(\beta_1 B_1 N-(\beta_1^2 I^*S^*+\kappa\beta_1\beta_2 D^*S^*)(\Upsilon_2-\Upsilon_1))I^*S^*(\Upsilon_2-\Upsilon_1)}{B_1B_2N^2-\beta_1^2 I^{*2}S^{*2}(\Upsilon_2-\Upsilon_1)}, 1\right)\right\},$$
$$u_3^* = \max\left\{0, \min\left(\frac{(\Upsilon_3-\Upsilon_4)I^*}{B_3}, 1\right)\right\}.$$

The optimal system is obtained by substituting $\hat{u}_1^*(t), \hat{u}_2^*(t)$, and $u_3^*(t)$ into the state equations (13) and costate equations (14), resulting in the optimal system (18).

$$
\begin{aligned}
\frac{dS^*}{dt} &= \Lambda - \frac{\beta_1(1-\hat{u}_1^*)(1-\hat{u}_2^*)I^* + \kappa\beta_2(1-\hat{u}_1^*)D^*}{N}S^* - \mu S^* + \theta R^*,\\
\frac{dE^*}{dt} &= \frac{\beta_1(1-\hat{u}_1^*)(1-\hat{u}_2^*)I^* + \kappa\beta_2(1-\hat{u}_1^*)D^*}{N}S^* - (\mu+\gamma+\omega)E^*,\\
\frac{dI^*}{dt} &= \gamma E^* - (\mu+\delta+\eta+u_3^*)I^*,\\
\frac{dR^*}{dt} &= \omega E^* + (\eta+u_3^*)I^* - (\mu+\theta)R^*,\\
\frac{dD^*}{dt} &= (\mu+\delta)I^* - \alpha D^*,\\
\frac{d\Upsilon_1}{dt} &= \Upsilon_1\left(\frac{\beta_1(1-\hat{u}_1^*)(1-\hat{u}_2^*)I^* + \kappa\beta_2(1-\hat{u}_1^*)D^*}{N} + \mu\right) - \Upsilon_2\left(\frac{\beta_1(1-\hat{u}_1^*)(1-\hat{u}_2^*)I^* + \kappa\beta_2(1-\hat{u}_1^*)D^*}{N}\right),\\
\frac{d\Upsilon_2}{dt} &= -A_1 - \Upsilon_1\left(\frac{\beta_1(1-\hat{u}_1^*)(1-\hat{u}_2^*)I + \kappa\beta_2(1-\hat{u}_1^*)D^*}{N}\right)\\
&\quad + \Upsilon_2\left(\frac{\beta_1(1-\hat{u}_1^*)(1-\hat{u}_2^*)I^* + \kappa\beta_2(1-\hat{u}_1^*)D^*}{N} + (\mu+\gamma+\omega)\right) - \Upsilon_3\gamma - \Upsilon_4\omega,\\
\frac{d\Upsilon_3}{dt} &= -A_2 + \Upsilon_1\left(\frac{\beta_1(1-\hat{u}_1^*)(1-\hat{u}_2^*)S^*N - (\beta_1(1-\hat{u}_1^*)(1-\hat{u}_2^*)I + \kappa\beta_2(1-\hat{u}_1^*)D^*)S^*}{N^2}\right)\\
&\quad - \Upsilon_2\left(\frac{\beta_1(1-\hat{u}_1^*)(1-\hat{u}_2^*)S^*N - (\beta_1(1-\hat{u}_1^*)(1-\hat{u}_2^*)I + \kappa\beta_2(1-\hat{u}_1^*)D^*)S^*}{N^2}\right) + \Upsilon_3(\mu+\delta+\eta+u_3^*)\\
&\quad - \Upsilon_4(\eta+u_3^*) - \Upsilon_5(\mu+\delta),\\
\frac{d\Upsilon_4}{dt} &= -\Upsilon_1\left(\frac{\beta_1(1-\hat{u}_1^*)(1-\hat{u}_2^*)I + \kappa\beta_2(1-\hat{u}_1^*)D^*}{N} + \theta\right) + \Upsilon_2\frac{\beta_1(1-\hat{u}_1^*)(1-\hat{u}_2^*)I^* + \kappa\beta_2(1-\hat{u}_1^*)D^*}{N}\\
&\quad + \Upsilon_4(\mu+\theta),\\
\frac{d\Upsilon_5}{dt} &= \Upsilon_1\frac{\kappa\beta_2(1-\hat{u}_1^*)S^*}{N} - \Upsilon_2\frac{\kappa\beta_2(1-\hat{u}_1^*)S^*}{N} + \Upsilon_5\alpha.
\end{aligned}
\tag{18}
$$

with initial conditions $S(0) = S_0, E(0) = E_0, I(0) = I_0, R(0) = R_0, D(0) = D_0$, and transversal conditions $\Upsilon_1(T) = \Upsilon_2(T) = \Upsilon_3(T) = \Upsilon_4(T) = \Upsilon_5(T) = 0$.

The optimal control analysis provides a mathematically rigorous justification for a central principle in infectious disease management: coordinated, multi-component interventions outperform isolated control measures. Although the optimization framework involves nonlinear dynamical systems and control-theoretic arguments, the resulting policy implications can be communicated in a concise and actionable form. The analysis indicates that the simultaneous application of three principal controls public health campaigns, case isolation, and enhanced treatment generates a synergistic effect, with the combined intervention achieving a substantially greater reduction in transmission than any individual component.

For public health decision-making, these results suggest a structured prioritization of resources prevention through awareness, containment through isolation, and mitigation through treatment. The analysis further demonstrates that both the timing and magnitude of controls critically influence their efficacy. Early, high-intensity implementation of combined interventions yields the greatest reduction in epidemic size and duration. This underscores the value of preparedness planning, rapid response infrastructure, and integrated health systems. In practical terms, the mathematical results indicate that allocating resources exclusively to a single intervention class is suboptimal, instead balanced investments across prevention, isolation, and treatment produce the most cost-effective and epidemiologically robust outcomes.

Overall, the optimal control results reinforce a foundational insight in mathematical epidemiology durable and effective outbreak containment requires simultaneous action along multiple transmission pathways, coordinated through well-designed, adequately resourced public health policies.

4. SIMULATION

In this section, we examine the controlled system described by Equation (9). Numerical simulations of the optimal control trajectories, using the parameter set listed in Table 3. Three alternative intervention strategies are evaluated to assess their effectiveness in mitigating the spread of Nipah virus disease. Numerical simulation results of the control problem using the forward-backward sweep method [16] with the help of the Matlab program. The combination of optimal control using two controls and three controls at once. Strategy 1 uses combination controls in the form of health campaigns on susceptible individuals and quarantine on infected individuals. Strategy 2 uses combination controls in the form of health campaigns on susceptible individuals and treatment on infected individuals. Strategy 3 uses combination

control in the form of quarantine and treatment of infected individuals. Strategy 4 uses combination controls in the form of health campaigns on susceptible individuals, quarantine and treatment on infected individuals. Comparison simulation of solutions with and without optimal control can be seen in Figures 3-7.

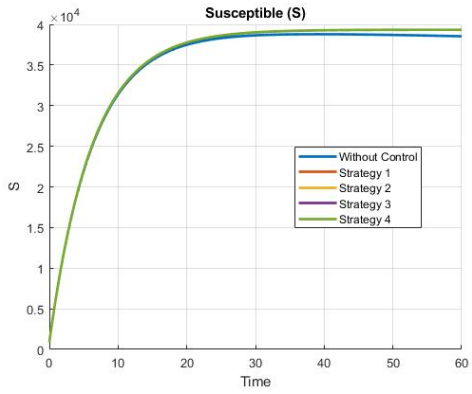

Figure 3: Susceptible individuals.

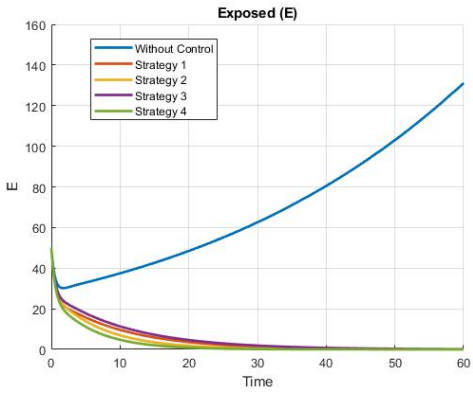

Figure 4: Exposed individuals.

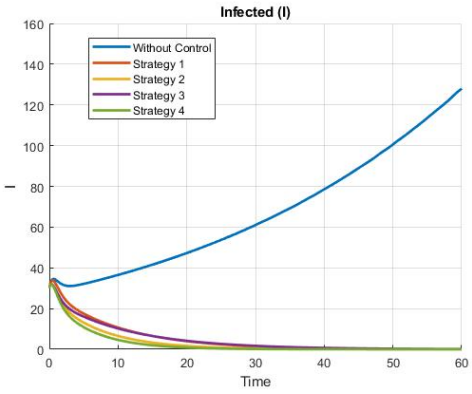

Figure 5: Infected individuals.

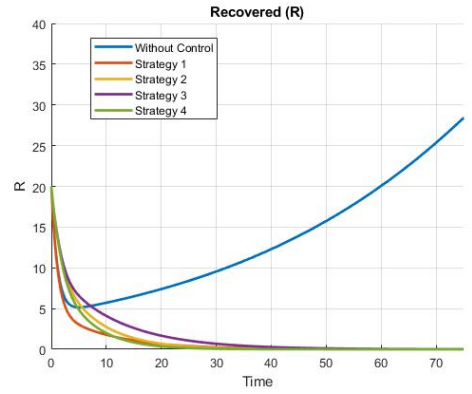

Figure 6: Recovered individuals.

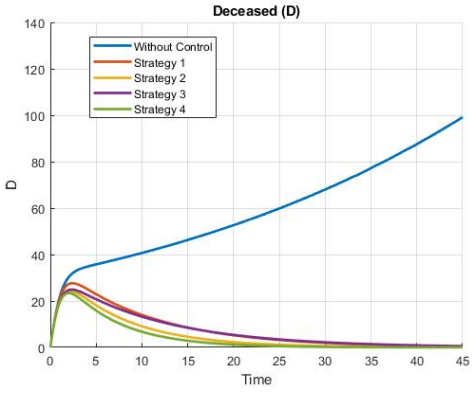

Figure 7: Deceased individuals.

The simulation results of the $SEIRD$ model, presented in Figures (3, 4, 5, 6, 7), illustrate substantial variation in the effectiveness of different control strategies against a Nipah virus outbreak. The scenario without any control results in a high and sustained number of infections and deaths, underscoring the critical need for proactive intervention. Strategy 1 which integrates health campaigns and quarantine, Strategy 2 which integrates health campaigns and treatment, Strategy 3 which integrates quarantine and treatment, achieves a markedly stronger impact by substantially lowering the exposed and infectious populations. However, the most effective and comprehensive outcome is obtained under Strategy 4, which combines health campaigns, quarantine, and treatment. This integrated approach drives infections and deaths close to zero in the shortest time while maintaining a large proportion of healthy individuals, demonstrating a synergistic interaction in which combined interventions outperform the sum of their individual effects.

From a policy perspective, these mathematical findings translate into clear and actionable guidance. Effective outbreak control depends on strategically modifying the model's most sensitive parameters through real-world interventions.

Reducing the transmission rate (β). The success of awareness campaigns in the model corresponds to public health initiatives aimed at lowering transmission probabilities. These include community education on avoiding contact with bats and sick animals, promoting hygiene practices such as regular handwashing, ensuring safe fruit consumption, and providing personal protective equipment (PPE) for healthcare workers and caregivers to minimize exposure risks.

Increasing the recovery rate (η) and reducing mortality (δ). Enhancing the treatment parameter in the model requires strengthening healthcare system capacity. This encompasses improving the training of healthcare personnel for rapid case detection, ensuring adequate supplies of supportive care equipment, and establishing dedicated treatment facilities to improve clinical outcomes and survival rates.

Isolating infectious individuals (ϕ_2). The quarantine parameter is operationalized through measures that facilitate rapid identification and isolation of suspected cases. This includes implementing clear operational protocols, maintaining specialized isolation wards, and conducting rigorous contact tracing to disrupt community transmission pathways.

In summary, no single intervention is sufficient to control a Nipah virus outbreak. Relying solely on public advisories or focusing exclusively on treatment will not achieve effective containment. The optimal strategy validated by the model is a coordinated, multi-component approach. Policymakers must simultaneously promote preventive behavior, isolate infectious individuals to halt transmission, and strengthen treatment capacity to reduce morbidity and mortality. This integrated policy framework, consistent with Strategy 4, offers the most efficient and reliable pathway for mitigating the health and societal consequences of a Nipah virus epidemic.

5. CONCLUSION

This study has established the stability dynamics of the Nipah virus transmission model, confirming that the disease-free equilibrium is asymptotically stable if $\mathcal{R}_0 < 1$, indicating that the disease can be eradicated, while the endemic equilibrium is stable if $\mathcal{R}_0 > 1$, signifying the disease will persist in the population. The sensitivity analysis identified that the parameters κ, β_1, and β_2 representing contact with infected individuals and corpses without protection—are the most influential on the spread of the virus. Consequently, the study demonstrates that a combination of control strategies (health campaigns, quarantine, and treatment), designed based on this sensitivity analysis, is not only effective in reducing infection rates but can also be optimized to minimize implementation costs. The optimal control formulation thus provides a strong basis for intervention prioritization by considering both epidemiological and economic impacts.

However, the transition of these model-based strategies from theory to practice requires a cautious acknowledgment of their limitations and the very real challenges of implementation. The model's assumptions of a homogeneous population and idealized control conditions often contrast with the complex social structures, cultural practices, and mobility patterns found in affected communities. In reality, enforcing strict quarantine may face public resistance and incur significant socioeconomic costs. The efficacy of health campaigns can be hampered by misinformation and logistical barriers in remote areas, while scaling up treatment is constrained by limited healthcare infrastructure. Therefore, while the model offers a crucial and optimal blueprint for action, its true utility lies in guiding the development of adaptable, context-specific, and resilient response plans. Ultimately, successfully controlling Nipah virus outbreaks depends not only on our mathematical understanding but also on our ability to address these practical challenges through robust public health systems, sustained community engagement, and strategic resource allocation.

ACKNOWLEDGEMENT

The author sincerely thanks Ministry of Higher Education, Science, and Technology of Republic Indonesia through the Center for Higher Education Funding and Assessment (PPAPT) for their generous support and facilitation in conducting this research. We would also like to express deep appreciation to the Indonesian Endowment Fund for Education (LPDP) Ministry of Finance of republic Indonesia and the Indonesian Education Scholarship (BPI) for financial support during this research. Their generous funding has enabled us to fulfill this work and contribute to the advancement of knowledge in this area.

REFERENCES

[1] Arunkumar, G., Chandni, R., Mourya, D.T., Singh, S.K., Sadanandan, R., Sudan, P. and Bhargava, B., Outbreak investigation of Nipah virus disease in Kerala, India, Journal of Infectious Diseases, 219(12), pp. 1867–1878, 2019.

[2] Banerjee, S., Niyas, V.K., Soneja, M., Shibeesh, A.P., Basheer, M., Sadanandan, R., Wig, N. and Biswas, A., First experience of ribavirin postexposure prophylaxis for Nipah virus during the 2018 outbreak in Kerala, India, Journal of Infection, 78(6), pp. 491–503, 2019.

[3] Boyce, W.E. and DiPrima, R.C., Elementary Differential Equations and Boundary Value Problems, New York: John Wiley and Sons, 2012.

[4] Brauer, F. and Castillo-Chavez, C., Mathematical Models in Population Biology and Epidemiology, New York: Springer, 2012.

[5] Chadha, M.S., Comer, J.A., Lowe, L., Rota, P.A., Rollin, P.E., Bellini, W.J., Ksiazek, T.G. and Mishra, A., Nipah virus-associated encephalitis outbreak, Siliguri, India, Emerging Infectious Diseases, 12(2), pp. 235–240, 2006.

[6] Ching, P.K., Reyes, V.C., Sucaldito, M.N., Tayag, E., Columna-Vingno, A.B., Fedelino Jr, F.M., Gilbert Jr, C.B., Sejvar, J.J., Eagles, D., Dueger, E., Kaku, Y. and Morikawa, S., Outbreak of henipavirus infection in the Philippines, 2014, Emerging Infectious Diseases, 21(2), pp. 328–331, 2015.

[7] Chitnis, N., Hyman, J.M. and Cushing, J.M., Determining important parameters in the spread of malaria through sensitivity analysis, Bulletin of Mathematical Biology, 70, pp. 1272–1296, 2008.

[8] Chua, K.B., Bellini, W.J., Rota, P.A., Harcourt, B.H., Tamin, A., Lam, S.K., Ksiazek, T.G., Rollin, P.E., Zaki, S.R., Shieh, W., Goldsmith, C.S., Gubler, D.J., Roehrig, J.T., Eaton, B., Gould, A.R., Olson, J., Field, H., Daniels, P., Ling, A.E., Peters, C.J., Anderson, L.J. and Mahy, B.W., Nipah virus: a recently emergent deadly paramyxovirus, Science, 288(5470), pp. 1432–1435, 2000.

[9] Diekmann, O. and Heesterbeek, J., Mathematical Epidemiology of Infectious Diseases: Model Building, Analysis, and Interpretation, Hoboken: Wiley, 2000.

[10] Gazal, S., Sharma, N., Tikoo, M., Shikha, D., Badroo, G.A., Rashid, M. and Lee, S., Nipah and Hendra viruses: deadly zoonotic paramyxoviruses with pandemic potential, Pathogens, 11(12), 1419, 2022.

[11] Goh, K.J., Tan, C.T., Chew, N.K., Tan, P.S., Kamarulzaman, A., Sarji, S.A., Wong, K.T., Abdullah, B.J., Chua, K.B. and Lam, S.K., Clinical features of Nipah virus encephalitis among pig farmers in Malaysia, The New England Journal of Medicine, 342(17), pp. 1229–1235, 2000.

[12] Gupta, N., Saurabh, S., Pradhan, S.K., Gupta, P. and Sharma, A., Nipah virus outbreak: a case study of the 2021 Kerala outbreak, Journal of Infectious Diseases Research, 5(2), pp. 112–118, 2021.

[13] Gurley, E.S., Hegde, S.T., Hossain, K., Sazzad, H.M., Hossain, M.J., Rahman, M., Sharker, M.A., Salje, H., Islam, M.S., Epstein, J.H., Khan, S.U., Kilpatrick, A.M., Daszak, P. and Luby, S.P., Convergence of humans, bats, trees, and culture in Nipah virus transmission in Bangladesh, Emerging Infectious Diseases, 23(9), pp. 1446–1453, 2017.

[14] Heffernan, J.M., Smith, R.J. and Wahl, L.M., Perspectives on the basic reproductive ratio, Journal of the Royal Society Interface, 2(4), pp. 281–293, 2005.

[15] Khan, M.Y., Ullah, S., Farooq, M., Al Alwan, B. and Saqib, A.B., Optimal control analysis for Nipah infection with vaccination and treatment, Nature Portfolio, 14, p. 17532, 2024.

[16] Lenhart, S. and Workman, J.T., Optimal Control Applied to Biological Models, New York: Chapman and Hall/CRC, 2007.

[17] Loyinmi, A.C. and Gbodogbe, S.O., Mathematical modeling and control strategies for Nipah virus transmission, EDUCATUM Journal of Science, Mathematics and Technology, 11(1), pp. 54–80, 2024.

[18] Luby, S.P., Rahman, M., Hossain, M.J., Blum, L.S., Husain, M.M., Gurley, E., Khan, R., Ahmed, B., Rahman, S., Nahar, N., Kenah, E., Comer, J.A. and Ksiazek, T.G., Foodborne transmission of Nipah virus in Bangladesh, Emerging Infectious Diseases, 12(12), pp. 1888–1894, 2006.

[19] Mondal, M.K., Hanif, M. and Biswas, M.H.A., SEI model for transmission of Nipah virus, International Journal of Modelling and Simulation, 37(3), pp. 185–197, 2017.

[20] Murray, J.D., Mathematical Biology I: An Introduction, New York: Springer-Verlag, 2002.

[21] Nikolay, B., Salje, H., Hossain, M.J., Khan, A.K., Sazzad, H.M., Rahman, M., Daszak, P., Stroher, U., Pulliam, J.R., Kilpatrick, A.M., Nichol, S.T., Klena, J.D., Sultana, S., Afroj, S., Luby, S.P. and Simpson, D., Transmission of Nipah virus: 14 years of investigations in Bangladesh, The New England Journal of Medicine, 380(19), pp. 1804–1814, 2019.

[22] Ozioko, A.L., Aja, R.O., Fadugba, S.E., Malesela, K. and Mbah, G.C.E., Optimal Nipah spread control dynamics, Communications in Mathematical Biology and Neuroscience, 2023(76), 2023.

[23] Patel, R., Kumar, A., Singh, R. and Jain, M., Re-emergence of Nipah virus outbreak in Kerala, India: lessons learned, Indian Journal of Epidemiology, 9(3), pp. 210–215, 2023.

[24] Paton, N.I., Leo, Y.S., Zaki, S.R., Auchus, A.P., Lee, K.E., Ling, A.E., Chew, S.K., Ang, B., Rollin, P.E., Umapathi, T., Sng, I., Lee, C.C., Lim, E. and Ksiazek, T.G., Outbreak of Nipah-virus infection among abattoir workers in Singapore, Lancet, 354(9186), pp. 1253–1256, 1999.

[25] Rahman, M.Z., Islam, A., Gurley, E.S., Hossain, M.J., Nahar, N., Sultana, R. and Luby, S.P., Outbreak of Nipah virus infection in Bangladesh, January–February 2023, Journal of Infectious Diseases, 227(5), pp. 890–898, 2023.

[26] Raza, A., Awrejcewicz, J., Rafiq, M. and Mohsin, M., Breakdown of a nonlinear stochastic Nipah virus epidemic model, Entropy, 23(12), 1588, 2021.

[27] Reddy, S., Rao, S. and Menon, V.K., Epidemiological investigation of the 2023 Nipah virus outbreak in Kerala, India, Journal of Public Health and Preventive Medicine, 11(4), pp. 275–281, 2023.

[28] Robinson, R.C., An Introduction to Dynamical Systems: Continuous and Discrete, Providence: American Mathematical Society, 2012.

[29] Sinha, D. and Sinha, A., Mathematical model of zoonotic Nipah virus in Southeast Asia, Acta Scientific Microbiology, 2(9), pp. 1–10, 2019.

[30] Sultana, J. and Podder, C.N., Mathematical analysis of Nipah virus infections using optimal control theory, Journal of Applied Mathematics and Physics, 4, pp. 1099–1111, 2016.

[31] World Health Organization, Nipah virus, 2021. https://www.who.int/news-room/fact-sheets/detail/nipah-virus, Accessed on May 21, 2024.

[32] Zewdie, A.D. and Gakkhar, S., A mathematical model of Nipah virus infection, Journal of Applied Mathematics, pp. 1–10, 2020.

[33] Zewdie, A.D., Gakkhar, S. and Gupta, S.K., Human-animal Nipah virus transmission: model analysis and optimal control, International Journal of Dynamics and Control, 11, pp. 1974–1994, 2023.